Tran. Natl. Acad. Sci. Azerb. Ser. Phys.-Tech. Math. Sci.
Mechanics, **44** (7), 29–40 (2024);
https://doi.org/10.30546/2706-7734.44.7.2024.28

Mathematical modeling of rectilinear cohesive transverse shear cracks in a fiber-reinforced composite reinforced with unidirectional fibers

Rafail K. Mekhtiyev

Received: 04.04.2024 / Revised:13.06.2024 / Accepted: 07.07.2024

Abstract. *Composite materials with two periodic circular holes, weakened by cohesive cracks, have a wide range of applications. From this point of view, the solution of longitudinal and transverse sliding problems in composite materials with such a geometric shape is of special interest. We consider an elastic medium (plane) weakened by a doubly periodic system of round holes filled with washers (linear fiber-reinforced) made of a homogeneous elastic material, the surface of which is covered with a uniform cylindrical film. The plane (binder) is weakened by two doubly periodic systems of rectilinear defects with broken bonds, located parallel to the abscissa and ordinate axes, and their sizes are not the same. General representations are constructed that describe a class of problems with a doubly periodic stress distribution outside circular holes and cracks in transverse shear. Analysis of the limit equilibrium of cracks in the framework of the end zone model is performed on the basis of a non-local failure criterion with a force condition for the advancement of the crack tip and a deformation condition for determining the advancement of the edge of the crack end zone.*

Keywords. Doubly periodic lattice · composite material · boundary conditions · transverse shear · linear algebraic equations · singular equations · cohesive cracks.

Mathematics Subject Classification (2010): 74S70, 65E05

1 Introduction

Currently, in many branches of modern technology, technical means in the form of perforated elements are used. In this regard, the development of methods for calculating the strength of perforated elements of machines and structures with cracks is of great importance. The study of these issues is important in connection with the development of energy, the chemical industry and other branches of technology, as well as the widespread use of materials with a doubly periodic structure (composites).

Rafail K. Mekhtiyev
Azerbaijan State Oil and Industry University, Baku, Azerbaijan E-mail: rafail60mehtiyev@mail.ru

A fairly complete picture of the characteristic stress distribution in the microstructure of linearly reinforced materials can be obtained by examining the shear stress distribution in a plane perpendicular to the fiber orientation. The solution of this problem opens up new possibilities for predicting the mechanical properties of composite materials according to the given initial characteristics for the constituent components and the type of microstructure.

2 Formulation of the problem

Let there be an elastic plane weakened by a doubly periodic system of round holes having radii λ $(\lambda < 1)$ and the centers of these holes are located at the points

$$P_{mn} = m\omega_1 + n\omega_2, \ \ (m, n = 0, \ \ \pm 1, \ \ \pm 2, \ ...,),$$

$$\omega_1 = 2, \ \ \omega_2 = \omega_1 h e^{i\alpha}, \ \ h > 0, \ \ \operatorname{Im} \omega_2 > 0.$$

Circular holes of the plane (binder) are filled with fibers (linear fiber-reinforced) from a homogeneous elastic material, the surface of which is uniformly covered with a homogeneous cylindrical film. The plane is weakened by two doubly periodic systems of rectilinear cracks with end zones with connections between the faces. Models of cracks with end zones were proposed [9] for brittle materials, and in [11, 5], models with end zones in the state of plastic flow at constant stress were considered.

The banks of shear cracks outside the end zones are free from external loads, and stresses $\sigma_x = 0$, $\sigma_y = 0$, $\tau_{xy} = \tau_{xy}^{\infty}$ (shear at infinity) act on the composite body.

Note that an increase in the external load on the continuation of the cracks will give rise to zones of pre-fracture. A crack model is used with connections between the edges in the end zones of pre-fracture. The end zones of cracks are modeled by areas with weakened interparticle bonds in the material. If, when the length of the crack tip is not small compared to the length of the crack, then methods for evaluating the fracture resistance of a material based on considering a crack with a small tip are not applicable. In these cases, it is necessary to simulate the stress state in the end zone of the crack taking into account the deformation characteristics of the bonds and the use of a two-parameter failure criterion that describes both the development of the crack tip and the change in the size of the end zone of the crack during its growth. If the processes of deformation and fracture in the end zones of cracks include several physical mechanisms, as, for example, in composite materials, then in such cases it is effective to use the model of the end zone with a singularity at the crack tip.

For homogeneous materials, such a model of a normal rupture crack was considered in papers [7, 6] and developed [10, 9] for cracks with an end region at the interface between materials with different properties.

The modeling of the end zones consists in considering them as part of the cracks and in the explicit application of cohesive forces to the surface of the cracks in the end zones, which restrain their shear. The dimensions of the end zones of cracks are considered to be commensurate with respect to the length of the cracks. The interaction between the edges of the end zones is modeled by introducing a pre-fracture zone between the edges of bonds with a given deformation diagram. The physical nature of such bonds and the size of the pre-fracture zones depend on the type of material. Under the action of an external load on a composite body in the bonds connecting the edge of the end zones of the cracks, tangential forces $q_x(x)$ and $q_y(y)$ will occur. These stresses are not known in advance and must be determined.

The problem of the stress-strain state of a composite piecewise-homogeneous medium is reduced to the construction in each of the areas occupied by the medium, two functions $\Phi(z)$ and $\Psi(z)$ according to given conditions on the boundaries of elastic media.

3 Method for solving the problem

$$\begin{array}{c}(\sigma_r - i\tau_{r\theta})\ _{b|\omega_m} = (\sigma_r - i\tau_{r\theta})\ _{t|\omega_m},\ \ (u+iv)\ _{b|\omega_m} = (u+iv)\ _{t|\omega_m},\\ (\sigma_r - i\tau_{r\theta})\ _{t|\Omega_m} = (\sigma_r - i\tau_{r\theta})\ _{s|\Omega_m},\ \ (u+iv)\ _{t|\Omega_m} = (u+iv)\ _{s|\Omega_m},\end{array} \tag{3.1}$$

on the edge of cracks with end zones

$$\begin{array}{c}(\sigma_y - i\tau_{xy})_s = f_x(x)\ \ parallel\ to\ the\ x-axis,\\ (\sigma_x - i\tau_{xy})_s = f_y(y)\ \ to\ the\ y-axis.\end{array} \tag{3.2}$$

Here, ω_m is the film–fiber interface; Ω_m is the film-plane interface in the cell with the number; m quantities related to the coating, fiber and plane, in the following are denoted respectively by the indices$t$, b, and s; $f_x(x) = 0$ on the free edge of the cracks; $f_x(x) = -iq_x(x)$ on the edge of the end zones of cracks; $f_y(y) = 0$ on the free edge of cracks parallel to the y-axis; $f_y(y) = -iq_y(y)$ to the edge of the end zones of the cracks.

The main ratios of the problem posed must be supplemented with ratios connecting the shear of the edge of the end zones of cracks and the forces in the bonds. Without loss of generality, we represent these equations in the form

$$\begin{array}{c}u^+(x,\ 0) - u^-(x,\ 0) = C\left(x,\ q_x(x)\right) q_x(x),\\ v^+(0,\ y) - v^-(0,\ y) = C\left(y,\ q_y(y)\right) q_y(y).\end{array} \tag{3.3}$$

Here, the functions $C\left(x, q_x(x)\right)$ and $C\left(y, q_y(y)\right)$ are the effective bond compliances; $(u^+ - u^-)$– shear of the edge of the end zones of cracks parallel to the abscissa axis; $(v^+ - v^-)$– shift of the edge of the end zones of cracks parallel to the y-axis.

The boundary conditions in the considered problem for finding complex potentials have the form [8]:

$$\begin{array}{c}\Phi_b(\tau_1) + \overline{\Phi_b(\tau_1)} - \left[\overline{\tau}\Phi'_b(\tau_1) + \Psi_b(\tau_1)\right]\ e^{2i\theta} =\\ = \Phi_t(\tau_1) + \overline{\Phi_t(\tau_1)} - \left[\overline{\tau}_1\Phi'_t(\tau_1) + \Psi_t(\tau_1)\right]\ e^{2i\theta},\end{array} \tag{3.4}$$

$$\begin{array}{c}-\|_b\overline{\Phi_b\left(\tau_1\right)} + \Phi_b\left(\tau_1\right) - \left[\overline{\tau}\Phi'_b\left(\tau_1\right) + \Psi_b\left(\tau_1\right)\right]\ e^{2i\theta} =\\ = \dfrac{\mu_b}{\mu_t}\left\{-\|_t\overline{\Phi_t\left(\tau_1\right)} + \Phi_t\left(\tau_1\right) - \left[\overline{\tau}_1\Phi'_t\left(\tau_1\right) + \Psi_t\left(\tau_1\right)\right]\ e^{2i\theta}\right\},\end{array} \tag{3.5}$$

$$\Phi_t(\tau) + \overline{\Phi_t(\tau)} - \left[\overline{\tau}\Phi'_t(\tau) + \Psi_t(\tau)\right]\ e^{2i\theta} = \Phi_s(\tau) + \overline{\Phi_s(\tau)} - \left[\overline{\tau}\Phi'_s(\tau) + \Psi_s(\tau)\right]\ e^{2i\theta} \tag{3.6}$$

$$\begin{array}{c}-\|_s\overline{\Phi_s(\tau)} + \Phi_s(\tau) - \left[\overline{\tau}\Phi'_s(\tau) + \Psi_s(\tau)\right]\ e^{2i\theta} =\\ = \dfrac{\mu_s}{\mu_t}\left\{-\|_t\overline{\Phi_t(\tau)} + \Phi_t(\tau) - \left[\overline{\tau}\Phi'_t(\tau) + \Psi_t(\tau)\right]\ e^{2i\theta}\right\},\end{array} \tag{3.7}$$

$$\Phi_s(t) + \overline{\Phi_s(t)} + t\overline{\Phi'_s(t)} + \overline{\Psi_s(t)} = f_x(t), \tag{3.8}$$

$$\Phi_s\left(t_1\right) + \overline{\Phi_s\left(t_1\right)} + t_1\overline{\Phi'_s\left(t_1\right)} + \overline{\Psi_s\left(t_1\right)} = f_y\left(t_1\right). \tag{3.9}$$

Here $\tau = \lambda e^{i\theta} + m\omega_1 + n\omega_2, m, n = 0, \pm1, \pm2, \ldots; \tau_1 = (\lambda - h)e^{i\theta} + m\omega_1 + n\omega_2 m, n = 0, \pm1, \pm2, ...$; h-coating thickness; t and t_1 are the affixes of the fracture edge points parallel to the abscissa and ordinate axes, respectively.

The boundary conditions can be simplified. It can be shown [1, 3] that the reduced system of equations will be as follows

$$\left(1 - \frac{\mu_t}{\mu_b}\right)\Phi_b\left(\tau_1\right) + \left(1 + \|_b\frac{\mu_t}{\mu_b}\right)\overline{\Phi_b\left(\tau_1\right)} -$$

$$-\left(1-\frac{\mu_t}{\mu_b}\right)\left[\overline{\tau}_1\Phi'_b\left(\tau_1\right)+\Psi_b\left(\tau_1\right)\right]e^{2i\theta}=\left(1+\|_t\right)\overline{\Phi_b\left(\tau_1\right)}, \tag{3.10}$$

$$\left(1-\frac{\mu_s}{\mu_t}\right)\Phi_t(\tau)+\left(1+\|_t\frac{\mu_s}{\mu_t}\right)\overline{\Phi_t(\tau)}-$$

$$-\left(1-\frac{\mu_s}{\mu_t}\right)\left[\overline{\tau}\Phi'_t(\tau)+\Psi_t(\tau)\right]e^{2i\theta}=\left(1+\|_s\right)\overline{\Phi_s(\tau)}. \tag{3.11}$$

Thus, it is necessary to determine three pairs of analytic functions $\Phi_t(z)$, $\Psi_t(z)$, $\Phi_b(z)$, $\Psi_b(z)$ and $\Phi_s(z)$, $\Psi_s(z)$, from the boundary conditions (4), (6), (8), (9), (10).

4 Solution of the boundary value problem

The solution of the boundary value problem (4), (6), (8)-(10) is sought in the form

$$\Phi_s(z)=\Phi_1(z)+\Phi_2(z)+\Phi_3(z),\ \ \Psi_s(z)=\Psi_1(z)+\Psi_2(z)+\Psi_3(z), \tag{4.1}$$

$$\Phi_b(z)=i\sum_{k=0}^{\infty}a_{2k}z^{2k},\ \ \Psi_b(z)=i\sum_{k=0}^{\infty}b_{2k}z^{2k}, \tag{4.2}$$

$$\Phi_t(z)=i\sum_{k=-\infty}^{\infty}g_{2k}z^{2k},\ \ \Psi_t(z)=i\sum_{k=-\infty}^{\infty}h_{2k}z^{2k}, \tag{4.3}$$

$$\Phi_1(z)=i\tau_{xy}^{\infty}+i\alpha_0+i\sum_{k=0}^{\infty}\alpha_{2k+2}\frac{\lambda^{2k+2}\rho^{(2k)}(z)}{(2k+1)!},$$

$$\Psi_1(z)=i\tau_{xy}^{\infty}+i\sum_{k=0}^{\infty}\beta_{2k+2}\frac{\lambda^{2k+2}\rho^{(2k)}(z)}{(2k+1)!}-i\sum_{k=0}^{\infty}\alpha_{2k+2}\frac{\lambda^{2k+2}S^{(2k)}(z)}{(2k+1)!}, \tag{4.4}$$

$$\Phi_2(z)=\frac{1}{2\omega}\int_{L_1}g(t)ctg\frac{\pi}{\omega}(t-z)dt,$$

$$\Psi_2(z)=-\frac{\pi z}{2\omega^2}\int_{L_1}g(t)\sin^{-2}\frac{\pi}{\omega}(t-z)dt,$$

$$\Phi_3(z)=-\frac{i}{2\omega}\int_{L_2}g_1\left(t_1\right)ctg\frac{\pi}{\omega}\left(it_1-z\right)dt_1, \tag{4.5}$$

$$\Psi_3(z)=-\frac{i}{2\omega}\int_{L_2}\Big\{g_1(t_1)ctg\frac{\pi}{\omega}(it_1-z)+\Big[ctg\frac{\pi}{\omega}(it_1-z)+$$

$$+\frac{\pi}{2\omega}(2t_1+iz)\sin^2\frac{\pi}{\omega}(it_1-z)\Big]g_1(t_1)\Big\}dt_1.$$

Here $g(t)$, $g_1(t_1)$ are the required functions.

$$g(x)=-\tfrac{2\mu_s i}{1+\|_s}\tfrac{d}{dx}\left[u^+(x,0)-u^-(x,0)\right],\ \text{on } L_1,$$

$$g_1(y)=\tfrac{2\mu_s}{1+\|_s}\tfrac{d}{dy}\left[\upsilon^+(0,y)-\upsilon^-(0,y)\right],\ \ \text{on } L_2, \tag{4.6}$$

$k_s=3-4v$ for plane strain, $k_s=\frac{(3-v)}{(1+v)}$ for plane stress state, v is the Poisson's ratio of the plane material, μ shear modulus, $\rho(z)=\left(\frac{\pi}{\omega}\right)^2\sin^{-2}\left(\frac{\pi}{\omega}z\right)-\frac{1}{3}\left(\frac{\pi}{\omega}\right)^2$, $S(z)$ is a special meromorphic function [123]; the integrals in (14)-(15) are taken along the lines $L_1 = \{[-l,-a]+[a,l]\}$; $L_2 = \{[-r,-b]+[b,r]\}$.

Additional conditions should be added to the basic integral representations, arising from the physical meaning of the problem

$$\int_{-l}^{-a} g(t)dt = 0,\quad \int_{a}^{l} g(t)dt = 0,\quad \int_{-r}^{-b} g_1(t_1)dt_1 = 0,\quad \int_{b}^{r} g_1(t_1)dt_1 = 0. \tag{4.7}$$

The unknown functions $g(t)$ and $g_1(t_1)$ and the coefficients a_{2k}, b_{2k}, g_{2k}, h_{2k}, α_{2k}, β_{2k} must be determined from the boundary conditions (4), (6), (8)-(10).

Applying the method of power series, we obtain the set of infinite linear algebraic equations

$$g_{2k}\lambda_1^{2k} = \left[\tfrac{\mu_b-\mu_t}{\mu_b(\|_t+1)}\right]\left\{(2k+1)a_{2k}\lambda_1^{2k} + b_{2k-2}\lambda_1^{2k-2}\right\},$$
$$g_{-2}\lambda_1^{-2k} = \left[\tfrac{\mu_b+\|_b\mu_t}{\mu_b(\|_t+1)}\right]a_{2k}\lambda_1^{2k}, \tag{4.8}$$

$$h_{-2k-2}\lambda_1^{2k-2} = (2k+1)a_{2k}\lambda_1^{2k} + b_{2k-2}\lambda_1^{2k-2} + \left[\frac{\mu_b-\mu_t}{\mu_b\left(\|_t+1\right)}\right](2k+1)a_{2k}\lambda_1^{2k} -$$
$$-\frac{\mu_b-\mu_t}{\mu_b\left(\|_t+1\right)}(2k-1)2ka_{2k}\lambda_1^{2k} - \frac{\mu_b-\mu_t}{\mu_b\left(\|_t+1\right)}(2k-1)b_{2k-2}\lambda_1^{2k+2},$$
$$h_{-2k-2}\lambda_1^{-2k-2} = a_{2k}\lambda_1^{2k} + \frac{\mu_b-\|_b\mu_t}{\mu_b\left(\|_t+1\right)}(2k+1)a_{2k}\lambda_1^{2k-2} -$$
$$-\frac{\mu_b-\mu_t}{\mu_b\left(\|_t+1\right)}\left\{(2k-1)a_{2k}\lambda_1^{2k} + b_{2k-2}\lambda_1^{2k+2}\right\},\quad (k=1,2,\ldots), \tag{4.9}$$

$$\frac{\mu_s\left(\|_t+1\right)}{\mu_t}ig_0 = -\left(\|_s+1\right)\left[i\sum_{j=0}^{\infty}\alpha_{2j+2}\lambda^{2j+2}r_{0,j} - i\tau_{xy}^{\infty} + A_0\right],$$

$$\left(1-\frac{\mu_s}{\mu_t}\right)(2k+1)ig_{-2k}\lambda^{-2k} - \left(1+\|_t\frac{\mu_s}{\mu_t}\right)ig_{2k}\lambda^{2k} -$$
$$-\left(1-\frac{\mu_s}{\mu_t}\right)ih_{-2k-2}\lambda^{-2k-2} = -\left(\|_s+1\right)\left(i\alpha_{-2k}+A_{-2k}\right),$$

$$i\left(g_2\lambda^2 - g_{-2}\lambda^{-2}\right) - ih_0 = -i\sum_{j=0}^{\infty}\alpha_{2j+2}\lambda^{2j+4}r_{1,j} - i\sum_{j=0}^{\infty}\beta_{2j+2}\lambda^{2j+2}r_{0,j} +$$
$$+i\sum_{j=0}^{\infty}(2j+2)\alpha_{2j+2}\lambda^{2j+2}s_{0,j} - i\tau_{xy}^{\infty} + A_0,$$

$$+i\sum_{j=0}^{\infty}\alpha_{2j+2}\lambda^{2j+2}r_{j,k}2k\lambda^{2k} + i\sum_{j=0}^{\infty}(2j+2)\alpha_{2j+2}\lambda^{2j+2}s_{k-1,j} + A_{2k},$$

$$i(2k+1)g_{-2k}\lambda^{-2k} - ig_{2k}\lambda^{2k} - ih_{2k-2}\lambda^{-2k-2} == i2k\lambda^{2k} - i\beta_{2j+2} + A_{-2k},$$

where $r_{j,k} = \frac{(2j+2k+1)!}{(2j)!(2k+1)!}\frac{g_{j+k+1}}{2^{2j+2k+2}}$, $r_{0,0}=0$, $s_{j,k} = \frac{(2j+2k+1)!}{(2j)!(2k+1)!}\frac{\rho_{j+k+1}}{2^{2j+2k+2}}$, $s_{0,0}=0$.

Requiring that functions (11) satisfy the boundary condition (8) on the edge of cracks with end zones, we obtain a system of two singular integral equations for the functions $g(x)$ and $g_1(y)$:

$$\begin{gathered} \frac{1}{\omega}\int_{L_1} g(t)ctg\frac{\pi}{\omega}(t-x)dt + H(x) = f_x(x), \\ -\frac{\pi}{\omega^2}\int_{L_2} g_1(t)\left[(t-y)sh^{-2}\frac{\pi}{\omega}(t-y)dt\right] + N(y) = f_y(y), \end{gathered} \tag{4.10}$$

$$H(x) = x\overline{\Phi'{}_s(x)} + \overline{\Psi_s(x)}, \Phi_s(x)\Phi_1(x) + \Phi_3(x),\ \ \Psi_s(x) = \Psi_1(x) + \Psi_3(x),$$

$$N(y) = \Phi_0(iy) + \overline{\Phi_0(iy)} + iy\overline{\Phi'{}_0(iy)} + \overline{\Psi_0(iy)}, \Phi_0(z) = \Phi_1(z) + \Phi_2(z),\ \ \Psi_0(z) = \Psi_1(z) + \Psi_2(z),$$

5 Numerical solution techique and analysis

Using the expansion of the functions $ctg\frac{\pi}{\omega}z$, $sh^{-2}\frac{\pi}{\omega}z$ in the main band of periods, the change of variables, as well as the quadrature formulas [7, 6, 9], we reduce the integral equations with additional conditions (17) to two finite algebraic systems with respect to the approximate values $p_k^0 = g^0(\eta_k)$, and $R_v^0 = g_1^0(\eta_k)$ of the desired functions at the points by chebyshev knots

$$\begin{cases} \sum\limits_{k=1}^{M} A_{m,k}p_k^0 + \frac{1}{2}H_*(\eta_m) = f_x(\eta_m)\,(m = 1, 2, ..., M-1)\,, \\ \sum\limits_{k=1}^{M} \frac{p_k^0}{\sqrt{\frac{1}{2}\left(1-\lambda_1^2\right)(\tau_k+1)+\lambda_1^2}} = 0, \end{cases} \tag{5.1}$$

$$\begin{cases} \sum\limits_{v=1}^{M} A_{m,v}R_v^0 + \frac{1}{2}N_*(\eta_m) = f_y(\eta_m)\,(m = 1, 2, ..., M-1)\,, \\ \sum\limits_{v=1}^{M} \frac{R_v^0}{\sqrt{\frac{1}{2}\left(1-\lambda_2^2\right)(\tau_v+1)+\lambda_2^2}} = 0. \end{cases} \tag{5.2}$$

The right side of the obtained systems (21), (22) includes unknown values of shear stresses $q_x\,(\eta_m)$ and $q_y\,(\eta_m)$ at the nodal points belonging to the end zones, respectively. Unknown stresses in bonds are determined from additional conditions (3). Using the constructed solution, we represent relations (3) in the form

$$\begin{gathered} \frac{d}{dx}\left[C\left(x, q_x(x)\right)q_x(x)\right] = -\frac{(1+\|_s)}{2\mu_s i}g(x), \\ \frac{d}{dy}\left[C\left(y,\ q_y(y)\right)q_y(y)\right] = \frac{(1+\|_s)}{2\mu_s}g_1(y). \end{gathered} \tag{5.3}$$

Requiring the fulfillment of conditions (23) at the nodal points belonging to the end zones of the cracks L_1 and L_2, respectively, we obtain two more systems of M_1 equations each for determining the values of $q_x(\eta_m)$ and $q_y(\eta_m)$ $(m = 1,\ 2,\ ...,\ M_1)$. In this case, the finite difference method is used.

The combined resolving system of equations (18), (19), (21), (22), (23) will be closed with respect to the unknowns p_k^0 $(k = 1, 2, ..., M)$, R_v^0 $(v = 1, 2, ..., M)$, α_{2k}, β_{2k}, A_{2k}, b_{2k}, h_{2k}, a_{2k}, g_{2k}, $q_x(\eta_m)$ and $q_y(\eta_m)$.

After determining the values of the functions p_k^0 and R_v^0, the stress intensity factors in the vicinity of the crack tips were found by the relations

$$K_{II}^a = -i\sqrt{\frac{\pi\updownarrow(1-\lambda_*^2)}{\lambda_*}}\frac{1}{2M}\sum_{k=1}^{M}(-1)^{k+M}p_k^0 tg\frac{\theta_k}{2},$$

$$K_{II}^{\updownarrow} = -i\sqrt{\pi\updownarrow\left(1-\lambda_*^2\right)}\frac{1}{2M}\sum_{k=1}^{M}(-1)^k p_k^0 ctg\frac{\theta_k}{2}, \tag{5.4}$$

$$K_{II}^{b} = -i\sqrt{\frac{\pi r\left(1-\lambda_2^2\right)}{\lambda_2}}\frac{1}{2M}\sum_{v=1}^{M}(-1)^{v+M} R_v^0 tg\frac{\theta_v}{2},$$

$$K_{II}^{r} = -i\sqrt{\pi r\left(1-\lambda_2^2\right)}\frac{1}{2M}\sum_{v=1}^{M}(-1)^{v} R_v^0 ctg\frac{\theta_v}{2}.$$

We note the limiting cases.

The material of inclusion, coating and binder is the same, i.e. $\mu_b = \mu_t = \mu_s, \|_b = \|_s = \|_t$.

From the given solution it follows

$$\Phi_1(z) = i\tau_{xy}^{\infty},\ \ \Psi_1(z) = i\tau_{xy}^{\infty},\ \ \Phi_b(z) = 0,\ \ \Psi_b(z) = 0,\ \ \Phi_t(z) = 0,\ \ \Psi_t(z) = 0,$$

then we get a solution for rows of cracks without holes.

At $\omega \to \infty$, general representations (11)–(15) give a solution to the problem for a single inclusion, uniformly covered with a homogeneous film, with cracks along the coordinate axes for the binder. To obtain a solution for a single hole with cracks, it is necessary to additionally take $\frac{\mu_b}{\mu_s} = 0$, $\frac{\mu_t}{\mu_s} = 0$.

To analyze the limit equilibrium of cracks with end zones, two conditions (two-parameter criterion) for failure are required. The first criterion is the condition of crack tip advancement, and the second one is the condition of breaking bonds at the edge of the end zone.

As the first failure condition, we use the Irwin force criterion for failure. The state of ultimate equilibrium of the crack tip corresponds to the fulfillment of the condition

$$K_{II} = K_{IIc}, \tag{5.5}$$

where K_{IIc} is the constant of the material, determined empirically [2, 4].

As the second failure condition, we use the criterion of the critical shift of the crack edges and consider that the breaking of bonds at the edge of the end zone ($x_* = \updownarrow - d \text{or} y_* = r - d_1$) occurs when the condition

$$V\left(x_*\right) = \sqrt{\left(u^+ - u^-\right)^2 + \left(v^+ - v^-\right)^2} = \delta_{cr}, \tag{5.6}$$

where δ_{cr} is the maximum bond length.

The solution of the system of algebraic equations (19), (21), (22), (23), (25) and (26) allows (for a given crack length and bond characteristics) to find the critical external load τ_{xy}^{∞} and the limit shift of the end zone in the state of the limit crack balance.

For given sizes of cracks and end zones, using the limiting values of K_{IIc} and δ_{cr}, it is possible to identify the modes of equilibrium and growth of cracks under monotonic loading. If conditions are met

$$K_{II} \geq K_{IIc},\ \ V\left(x_*\right)\ \text{ and }\ V\left(y_*\right) < \delta_{cr},$$

then the crack tip advances with a simultaneous increase in the length of the end zone without breaking the bonds. This stage of crack development can be considered as a process of adaptability to a given level of external loads.

Crack tip growth with simultaneous rupture of bonds at the edge of the end zone will occur when conditions $K_{II} \geq K_{IIc}$, $V\left(x_* \text{ or } y_*\right) \geq \delta_{cr}$ are met.

So, for example, if the conditions $K_{II} < K_{IIc}$, $V\left(x_* \text{ or } y_*\right) \geq \delta_{cr}$ the bonds are broken without crack tip advancement, and the size of the end zone is reduced, tending to a critical value for a given load level. When the conditions are met $K_{II} < K_{IIc}$, $V\left(x_* \text{ and } y_*\right) < \delta_{cr}$ the positions of the crack tip and end zone will not change.

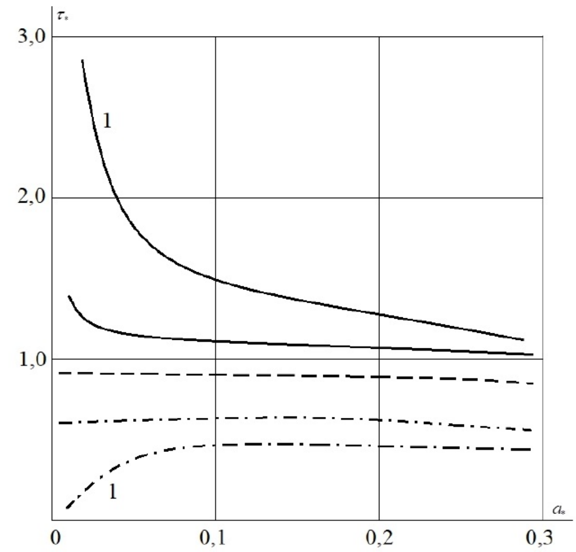

Fig. 1. Dependences of the critical load $\tau_* = \frac{\tau_{xy}^{\infty}\sqrt{\omega}}{K_{IIc}}$ on the distance $a_* = a - \lambda$ for both ends of the crack at $\lambda = 0,3$

Based on the results obtained in Fig. 1. in the case of a rigid inclusion at $v_s = 0,3$, graphs of the dependence of the critical load $\tau_* = \frac{\tau_{xy}^{\infty}\sqrt{\omega}}{K_{IIc}}$ on the distance $a_* = a - \lambda$ for both ends of the crack are plotted along the abscissa axis (curve 1 corresponds to the left end) at $\lambda = 0,3$. For comparison, the dashed line shows dependence τ_* in the absence of inclusions and coatings (the material of the inclusion, coating, and binder is the same) with the same fracture geometry, calculated by the described method. In the same place, the dash-dotted line shows the dependence in the case of an absolutely flexible inclusion (the holes are not filled with anything). For any elastic inclusion, the stress state pattern will occupy an intermediate position between these two limiting cases.

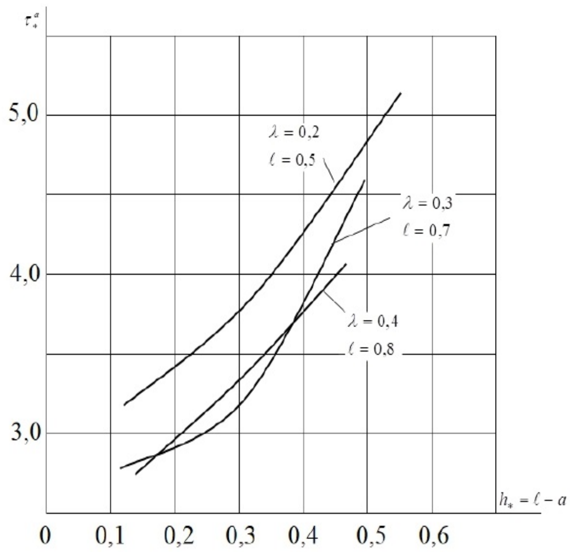

Fig. 2. Dependences of the ultimate load $\tau_*^a = \frac{\tau_{xy}^{\infty}\sqrt{\omega}}{K_{IIc}}$ on the length $h_* = \updownarrow - a$ of the crack

Fig. 2 and 3 show graphs of the dependence of the ultimate load τ_* on the length of the crack. In the calculations, $\frac{\mu_b}{\mu_s} = 25$; $\frac{\mu_b}{\mu_t} = 50$. were taken.

As can be seen, for some values of the hole radius, a stable development of a system of cracks (their mutual strengthening) is possible. The parametric analysis of the problem showed that the stress concentration near the inclusions in the binder has a significant effect on the development of very small cracks. With an increase in the length of cracks with end zones, this effect fades and can be neglected already at $\updownarrow - \lambda > \lambda$ and$r - \lambda > \lambda$, but in this case, the interaction of cracks begins to affect. Depending on the geometric and physical parameters of the problem, a stable development of cracks with end zones is observed.

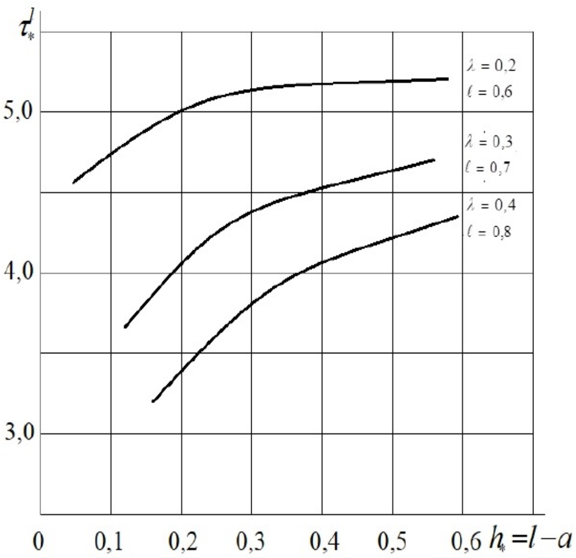

Fig. 3. Dependence of ultimate load $\tau_*^{\updownarrow} = \frac{\tau_{xy}^{\infty}\sqrt{\omega}}{K_{IIc}}$ on crack length $h_*= \updownarrow - a$

The presence of a flexible inclusion increases the stress intensity factor, while rigid inclusions reduce it compared to the binder material.

The influence of the inclusion is especially effective on the closely spaced crack tip.

Thus, the analysis shows that the magnitude of the external load τ_{xy}^{∞} and the critical parametersK_{IIc}, δ_{cr}determine the nature of the destruction:

1) growth of the crack tip with the advancement of the end zone;

2) reduction in the size of the end zone without growth of the crack tip;

3) growth of the crack tip with simultaneous rupture of bonds at the edge of the end zone.

The model of a crack with end zones makes it possible to study the patterns of force distribution in bonds under various deformation laws, to analyze the limit equilibrium of cracks taking into account the deformation and force fracture criteria, and also to predict the critical external load and crack resistance of a composite body (composite). It is possible to choose a system of concentrators (inclusions) in such a way that the stress field created by them will slow down the development of cracks in the binder.

Consider the case where the material of the cylinder is Lucite and the fluid is water and assume that $h/R = 0.2$. Here we consider the dispersion curves related to the lowest mode and generated for different values of the p/μ ratio. Note that the dispersion diagrams of the first lowest mode have two branches, conditionally called the left and right branches. Here we consider the left and right branches of this mode, constructed for different values of p/μ and shown in Fig. 1. Note that in Fig. 1, the graphs grouped with the letter a refer to the left branches, while the graphs of the right branches are grouped with the letter b. The ZGV points resulting from the condition $d(\omega R/c_2)/d(kR) = 0$ are also indicated in these graphs.

From the analysis of these diagrams, it can be seen that an increase in the values of the p/μ ratio leads to a decrease (increase) in the wave frequency and the dimensionless wave number in relation to the ZVG points on the dispersion diagrams related to the left (right) branches of the first lowest mode.

6 Conclusions

Thus, in the present work, the influence of the magnitude of the initial inhomogeneous stresses in the cylinder immersed in the fluid on the frequency and the dimensionless wave number of the ZGV points in the dispersion diagrams of the first lowest mode was investigated. The investigations are carried out using the so-called linearized 3D equations and relations of the theory of elastic waves in bodies with initial stresses to describe the motion of the cylinder and using the linearized Euler equations to describe the flow of the compressible barotropic inviscid fluid. The corresponding mathematical problem is solved by applying the discrete analytical method and the corresponding dispersion equation is obtained, which is solved numerically. As a result of this solution, the dispersion diagrams of the first lowest mode are obtained for different values of hydrostatic pressure causing the initial stresses in the cylinder. The specific numerical results are obtained for the case when the cylinder material is Lucite and the fluid is water. As a result of analyzing these results, it is found that the ZGV points appear on the dispersion diagrams and these diagrams have two branches: a left and a right branch. It is also found that when the hydrostatic pressure values are increased, the frequency and the dimensionless wave number with related to the ZGV points on the left (right) branches of the dispersion diagrams decrease (increase) monotonically

References

1. Birger, I.A.: General algorithms for solving elasticity, plasticity and creeping problems. *In Achievements of Deformed Medium Mechanics, Nauka, Moscow*, pp. 51-73 (in Russian) (1975).
2. Cherepanov, G.P.: Mechanics of Brittle Fracture. *Nauka, Moscow*, 1974 (in Russian).
3. Gol'dshtein, R.V., Perel'muter, M.N.: *The way to simulate crack growth resistance for composite materials*. Vychisl. Mekh. Sploshnykh Sred, **2** (2), pp. 22-39 (2009) (in Russian).
4. Il'yushin, A.A.: Plasticity. *Logos, Moscow*, (2004) (in Russian).
5. Ishlinsky, A.Yu., Ivlev, D.D.: The Mathematical Theory of Plasticity. *Fizmatlit, Moscow*, (2001) (in Russian).
6. Kalandiya, A.I.: *On the approximate solution of one class of singular integral equations*. Dokl. Akad. Nauk SSSR, **125** (9), pp.715-718 (1959) (in Russian).
7. Mehtiyev, R.K.: Longitudinal shift of bodies with complex structure, relaxed rectified through crack. Proc. of the 7th Intern. Conf. Control and Optimization with Industrial Applications (COIA), 1, August 26-28, 2020, Baku, Azerbaijan, pp. 281-283.
8. Mekhdiev, A.K., Mekhtiev, R.K.: *Transverse shear of an isotropic elastic medium in the case when the binder and inclusions are weakened by crack initiation*. Baku Mathematical Journal, **1** (2), (2022) pp. 125-144.
9. Mirsalimov, V.M.: Multidimentional Elastic-Plastic Problems. *Nauka, Moscow*, (1987) (in Russian).

10. Muskhelishvili, N.I.: Some Basic Problems of Mathematical Theory Elasticity. *Kluwer, Amsterdam*, (1977).
11. Panasyuk, V.V. Mechanics of Quasibrittle Fracture of Materials. *Naukova Dumka, Kiev*, (1991) (in Russian).